INTERNATIONAL JOURNAL OF HYDROGEN ENERGY XXX (2015) 1–13

Available online at www.sciencedirect.com

ScienceDirect

journal homepage: www.elsevier.com/locate/he

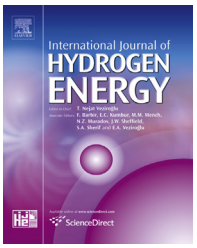

Ni–Co bimetallic catalyst for hydrogen production in sewage treatment plants: Biogas reforming and tars removal

M. Benito [a,*], I. Ortiz [a], L. Rodríguez [b], G. Muñoz [b]

[a] Centro de Investigaciones Energéticas Medioambientales y Tecnológicas (CIEMAT), Av. Complutense 40, 28040 Madrid, Spain

[b] Institute of Catalysis and Petrochemistry CSIC C/ Marie Curie s.n., 28049 Madrid, Spain

ARTICLE INFO

Article history:
Received 13 March 2015
Received in revised form
22 June 2015
Accepted 30 June 2015
Available online xxx

Keywords:
Hydrogen
Catalyst
Sewage treatment plants
Biogas
Energy valorisation
Tar

ABSTRACT

A Ni–Co bimetallic catalyst supported on lanthana promoted alumina was prepared by excess volume solution method. The catalyst was characterised by XRD, N_2 adsorption isotherms, XRF, TPO, SEM and XPS. The catalyst was tested in a simulated biogas stream with a CH_4:CO_2 1:1, usually presented after anaerobic digestion in sewage treatment plants, and in a simulated air gasification stream containing toluene as a tar model compound.

The catalyst was submitted to catalytic activity *vs.* temperature tests in order to determine the optimum temperature to maximize conversion and selectivity in both processes.

At 700 °C, equilibrium conversion in the case of biogas conversion was achieved, and total toluene and methane conversion in gasification stream was reached, maximizing hydrogen production with the lack of complex tar by-products formation.

Long-term reaction experiments up to 100 h demonstrated the stability of catalyst performance. Post-reaction characterisation of catalytic samples by SEM-EDX and XPS revealed the lack of coke deposits on the catalyst, responsible of catalyst deactivation in the most of catalytic systems reported in the literature.

At the light of the results obtained, the catalyst developed could be applied to produce renewable hydrogen from anaerobic digestion units of sewage plants, through the energy valorisation of biogas stream and sludge gasification.

Introduction

The energy valorisation of industrial and municipal sewage has until recently been mainly conducted using two methods: anaerobic digestion and incineration with energy recovery. Anaerobic digestion has the advantage of reducing the dry mass of sludge and produces a methane rich biogas stream that can be used as a fuel. As a process by-product, sludge with a residual organic matter is obtained.

* *Corresponding author*. Tel.: +34 913466701; fax: +34 915854760.
E-mail address: mj.benito@ciemat.es (M. Benito).

http://dx.doi.org/10.1016/j.ijhydene.2015.06.163

Furthermore, residual energy from sludge gasification can be also obtained.

Nowadays biogas represents the highest electricity capability production among renewables scenario. It is a remarkable fact that biogas production in Europe by 2011 represented 10.1 Mtoe, this means 35.9 TW h of electricity generated [1].

The biogas produced in anaerobic digestion has been used frequently in spark ignition gas engines or dual fuel engines with an efficiency range in terms of chemical energy conversion to electricity of 35–42% [2]. However, the high concentration of CO_2 presented (40–50%) limits energy efficiency and can produce ignition problems in this type of engines. From this point of view, biogas valorisation into hydrogen, represents an alternative and environmental friendly option when fuel cells are selected as a high efficient energy conversion system [3–6].

Biogas streams can be converted directly into hydrogen using the CO_2 present in biogas streams as an oxidant to perform the reforming reaction [7–11]. Among technical options for biogas valorisation into hydrogen, the direct reforming of methane with carbon dioxide with an external biogas combustion to generate the heat necessary to support the reaction enthalpy, is the optimum strategy to minimize the cost of hydrogen production [12]. Taking into account the state of the art, the development of catalysts able to overcome deactivation processes mainly due to coke deposition, is the key for applying this emergent technology [13]. Many papers have been the published concerning to the development of catalysts resistant to poisoning by carbon formation, publishing several reviews of the state of the art [14–16].

Nickel, iron and cobalt-based catalysts are quite active in methane decomposition reaction. Tokunaga et al. [17] performed the initial researches studying the activity of the Group VIII (Fe, Co and Ni) first transition metals series using silica and alumina as support, resulting Ni and Co the most active. The problem to overcome is to control activity due to this type of catalysts are capable of activating C–C and C–H bonds to form coke [18,19]. The coke produced blocks active sites of catalysts leading to its deactivation. However, the catalyst active phase is not only the key factor to design an active and stable catalyst. The properties of the support strongly affect the catalyst activity due to the variation in surface area and acid–base properties. From this point of view, the adsorption and dissociation of CO_2 is favoured by basic supports. Gadalla et al. [20] studied Ni catalysts on different supports, concluding that Al_2O_3, Al_2O_3–MgO–CaO and Al_2O_3 have a higher activity than Al_2O_3–SiO_2 (experiencing rapid deactivation), and that the supports containing MgO and CaO were stable.

Taking into consideration the increase of anaerobic digestion processes in waste water treatment plants, the production of sewage sludge (by-product) has increased worldwide in recent years, so environmentally friendly treatment of sewage sludge has become an important issue [21]. Energy valorisation of sewage sludge by gasification reduces the waste volume while a part of the energy contained in it is recovered. The main drawback for this technology is the high tar content in the gasification gas streams. Tar are defined in the Technical Specification CEN/TS 15439 as all organic compounds presented in the gasification product gas excluding gaseous hydrocarbons (C1–C6). Tar can condense when the temperature is below the dew point or can be polymerize or adsorbed in fine particles producing soot. All these processes produce dirty, corrosion and plugging in pipes, filters and engines with great costs in maintenance as well as loss of energy efficiency which limits seriously gasification application [22]. Current removal methods, based on physical (filtration) o chemical processes (solvents treatment) are not satisfactory enough for tar removal [23]. On one hand, these methods simply transfer tar compounds from gas stream to the solvent or to the solids used as filtration system, producing highly pollutant and hazardous waste, which must usually be managed as a toxic and dangerous waste. On the other hand, these methods operate at low temperatures, and require the gas to be cooled down which implies a decrease in energy efficiency of the integrated system.

From this point of view, tar cracking and reforming methods are an attractive choice to reduce the concentration of tar in the gasification product gas stream because of tar can be destroyed through reactions at high temperature immediately downstream the gasifier without creating a waste liquid stream [24,25]. Among the processes for tar removal at high temperature, is the tar catalytic cracking, process carried out at temperatures above the gasifier operation temperature (>1000° C), the most used, being rapid deactivation of catalysts due to the formation of coke the main limitation. These poly-aromatic species (tar) block catalytic active sites. The limiting stage for the development of gasification technology is synthesizing stable catalysts resistant to poisoning by coke and minor components produced in biomass gasification such as H_2S, capable of ensuring a long-term operation, and which maximize selective conversion of tar towards valuable products in synthesis gas production, primarily CO and H_2.

Many efforts have been done to develop catalysts with enough activity and stability to perform tar reforming based on natural minerals such as olivine [26,27], dolomite [28,29], or synthetic catalysts supported on alumina, silica using different active phase i.e. nickel, cobalt and precious metals.

Zhang et al. [29] studied the performance of nickel catalysts supported on silica for catalytic cracking of tars at 550° C. The catalyst activity was maintained for a short period due to the formation of large amounts of coke on the catalyst surface, phenomenon also described by Aznar [30] and Baker [31].

Lamacz et al. [32,33] tested Ni catalysts supported on Ce–Zr mixed oxide, using toluene and 1-methyl naphthalene as tar model compound. The catalyst activity was very good in the case of toluene and worse in the case of 1-methyl naphthalene to become starting at 500° C, reaching a conversion of 99% at 800° C in the case of toluene, and 88% in for 1-methyl naphthalene. The catalyst performance key focuses on the ability of the catalyst to supply oxygen network.

Alumina supported catalysts have been extensively studied using precious metals such as Pt as active phase and transition metals such as Ni [34,35].

Please cite this article in press as: Benito M, et al., Ni–Co bimetallic catalyst for hydrogen production in sewage treatment plants: Biogas reforming and tars removal, International Journal of Hydrogen Energy (2015), http://dx.doi.org/10.1016/j.ijhydene.2015.06.163

Several authors have tried to modify nickel catalysts by using promoters to minimize the formation of coke. Dou et al. [36] conducted a study based in five catalysts, being zeolite-Y and NiMo catalysts the most effective, reaching 100% conversion at 550° C. In their experiments detected small amounts of coke after 168 h reaction.

Taking into consideration biogas reforming and tar removal in sewage gasification processes, the catalytic systems studied in literature and the causes of catalyst deactivation were similar, this is the reason why in this paper we propose a single catalyst for both processes to overcome coke deposition problems maximising hydrocarbon conversion.

The aim of this work is to study the catalytic activity and stability of a new Ni–Co bimetallic catalyst applied to biogas conversion and tar removal, processes integrated in sewage treatment plants for energy recovery by hydrogen production. Post-reaction samples analysis by means of TPO, XPS and SEM are the characterisation techniques used to support the results obtained in reaction conditions.

Experimental

Catalysts preparation

The catalyst was prepared by impregnation in excess dissolution method. A one step impregnation method was used to deposit the active phase and promoter on aluminium oxide (Sasol Disperal). The nominal composition of the active phase was 5%wt Ni and 3%wt Co. Aqueous solutions of $Ni(NO_3)_2 \cdot 6H_2O$, $Co(NO_3)_2 \cdot 6H_2O$, $La(NO_3)_2 \cdot 6H_2O$ (Panreac) were used as precursor salts respectively. An excess of aqueous solution of metal precursor salts was added to alumina oxide powder, calcined previously at 800 °C for 4 h, in a rotary vacuum evaporation system. After impregnation, the catalyst was dried in air (110 °C, 12 h) and then calcined at 800 °C for 4 h in order to remove precursor salts and to stabilize the active phase, trying to avoid active phase sintering due to the increase of temperature and loss of surface area in reaction conditions. The aim is to stabilize the catalyst texture prior to reaction trying to avoid or to minimize surface area loss in reaction conditions that could produce changes in catalyst activity and stability.

Catalysts characterization

Textural analysis was performed by N_2-adsorption isotherms obtained at 77 K for alumina support calcined at 800 °C and catalyst sample synthesized. The equipment used was a Micromeritics model ASAP 2020. Prior to analysis, the samples were degassed at 473 K for 24 h to remove the physically adsorbed moisture from catalyst surface. BET equation was used for adjusting the adsorption isotherms in order to calculate the specific surface area of the support and catalyst sample. Other parameters such as porosity, pore distribution were also determined.

Chemical composition of the fresh catalytic sample after calcination at 800 °C was obtained by X Ray Fluorescence with a X Ray fluorescence spectrometer PANALYTICAL AXIOS/Perladora PERL X'3 PANALYTICAL.

XRD patterns of the support and prepared catalyst were obtained on 1 cm^3 powder samples in a diffractometer X'PERT PRO PANALYTICAL. Measures were performed at 2θ range of 2–100°, using CuKα radiation (λ = 1.540598 Å) and removing Kβ radiation by a nickel filter, with a $0.05° \cdot s^{-1}$ scanning, and an accumulation time of 2 s. Crystalline phases were identified by X'PERT HIGHSCORE PLUS software, comparing the patterns obtained to PDF-2 data base of the Joint Committee on Powder Diffraction Standards JCPDS 2013.

Temperature programmed oxidation (TPO) analyses of catalyst samples after reaction, were carried out using a METTLER-TOLEDO TGA/SDTA 851 thermo-balance, in order to determine the amount of carbon deposited on catalysts. The standard protocol involved the weight change of samples (100 mg) in a quartz pan during its heating in 50 mL $N \cdot min^{-1}$ of N_2 flow as purge gas, and 21% O_2–79% N_2 (50 mL $N \cdot min^{-1}$) as reactive gas from 25 to 1000 °C at a heating rate of 10 °C min^{-1}. TG system is connected to a mass spectrometer PFEIFFER THERMOSTAR, in order to record the evolution of the m/z ascribed to different reaction products desorbed in the oxidation reaction.

Scanning electron microscopy (SEM) images of the catalysts were obtained with a HITACHI-S2500 microscope at magnification ×100, ×200, ×500, ×4000, and HV of 25 kV. EDX analyses on different positions in every catalyst sample were performed in order to obtain the chemical composition. A Mapping of every compound identified in every catalyst sample was obtained to get information about possible segregation phenomena.

XPS spectra of fresh catalytic samples and submitted to reaction conditions during 100 h were obtained with a Perkin–Elmer PHI 5400 spectrometer equipped with a hemispherical electron analyzer and a Mg K_α anode (1253,6 eV). Intensities were estimated by calculating the integral of each peak after smoothing and subtraction of the S-shaped background and fitting of the experimental curve to a mixture of Lorentzian and Gaussian lines of variable proportions.

Activity tests

Methane reforming with CO_2, and toluene reforming reaction experiments were carried out in a microactivity reaction equipment (Fig. 1) with a fixed-bed tubular quartz flow reactor (3/8″ o.d., 330 mm length) operating isothermally and at atmospheric pressure. Catalyst samples (50 mg, grain size of 0.42–0.50 mm for dry methane reforming, and 1750 mg for toluene reforming with the same grain size) were mixed with inert diluter (SiC) in 1:4 weight ratio.

Biogas simulated stream consisted in 100 mL $N \cdot min^{-1}$ with a CH_4:CO_2 ratio 1:1. In the case of a simulated sewage sludge fluidised bed gasification, the composition of the gas stream was 11% H_2, 48.1% N_2, 17.7% CO_2, 3.4% CH_4, 7.8% CO, 12.1% H_2O and 25 g m^{-3} of toluene, being the total flow 105 mL $N \cdot min^{-1}$.

Two types of reaction experiments were performed: conversion/products distribution *vs.* temperature, and *vs.* time at reaction temperature selected.

Gases were fed to reaction system by means of mass flow controllers with nominal flow range of 100 mL $N \cdot min^{-1}$. H_2O

Please cite this article in press as: Benito M, et al., Ni–Co bimetallic catalyst for hydrogen production in sewage treatment plants: Biogas reforming and tars removal, International Journal of Hydrogen Energy (2015), http://dx.doi.org/10.1016/j.ijhydene.2015.06.163

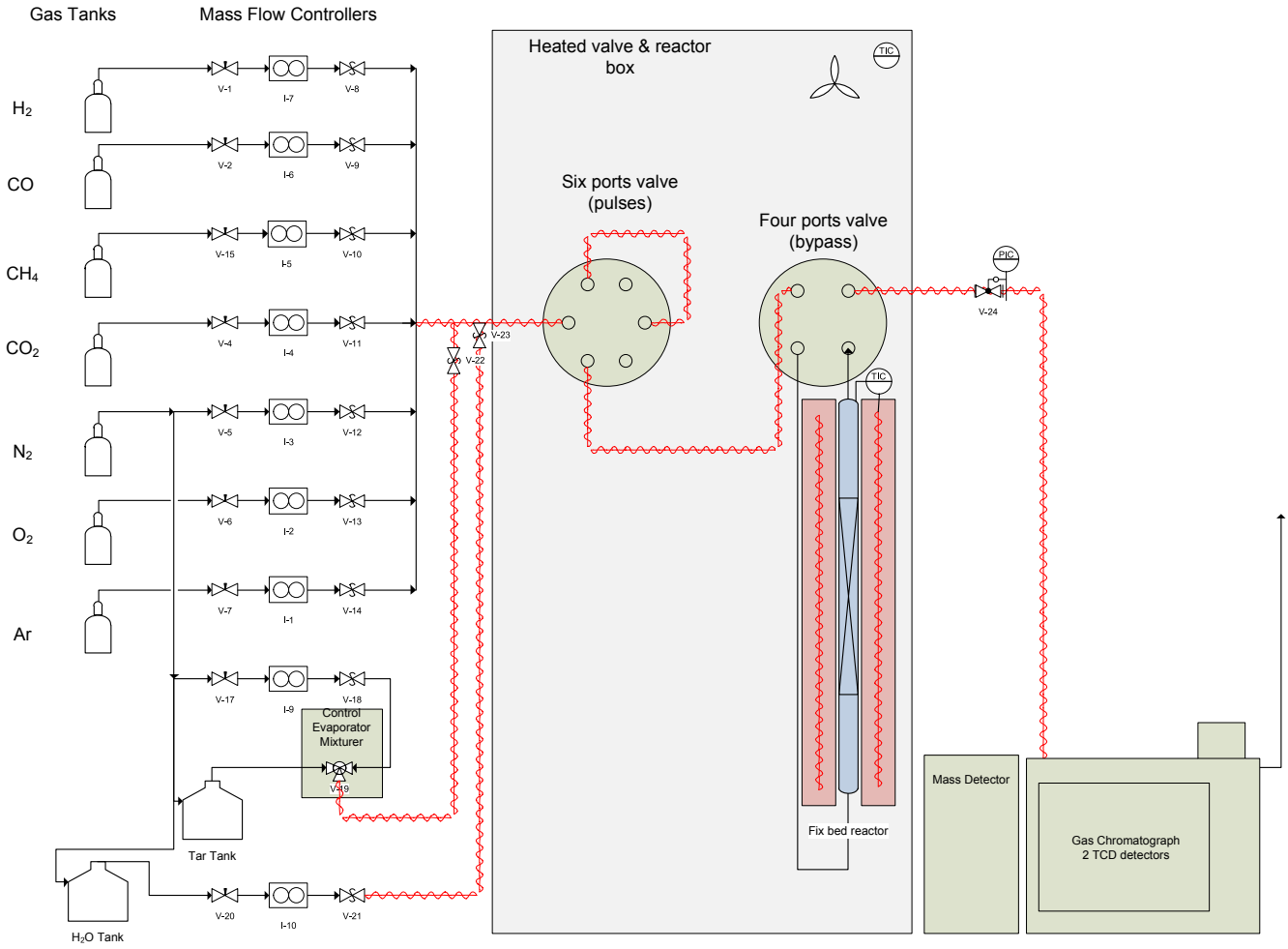

Fig. 1 – Scheme of the microactivity test system.

was fed to the system using a liquid mass flow controller with nominal range of 10 g min^{-1}, and finally, toluene was fed to the reactor by means of a CEM (control evaporation mixture system) where gaseous stream is mixed controllably with toluene, in a mass flow range of 0–2 g min^{-1}. All mass flow controllers were manufactured by Bronkhorst.

An SCADA system allows acquiring and controls the reaction temperature, pressure, gas and liquid flows.

The reaction products were analysed with an AGILENT 7890A chromatograph connected on line and equipped with two TCD and 5975C Mass detectors. Helium was used as carrier gas.

Methane, carbon dioxide and toluene conversion, denoted as X_{CH4}, X_{CO2} and $X_{toluene}$ respectively, and the effluent gas composition, denoted as C_i, were calculated according to Eqs. (a) and (b), respectively.

$$X_i(\%) = \frac{\text{moles}_{i-in} - \text{moles}_{i-out}}{\text{moles}_{i-in}} \cdot 100 \quad \text{(a)}$$

$$C_i(\%) = \frac{\text{moles } P_i}{\sum_{i=1}^{n} \text{moles } P_i} \cdot 100 \quad \text{(b)}$$

where P_i is the molar amount of products.

Results and discussion

Catalysts characterization

N_2 adsorption–desorption isotherms at 77 K were obtained for alumina support and catalyst sample synthesized respectively. The isotherm obtained for Disperal alumina support presents a hysteresis cycle typical of a mesoporous solid, that corresponds to IV H3 type (IUPAC classification) ascribed to mesoporous solids that presents capillary condensation without adsorption limitation, usually presented in laminar pores. The impregnation of the active phase (Ni and Co) and promoter (La) produce a slight decrease of specific surface area, pore volume and pore size (Table 1) produced by a partial blockage of the alumina pores by precursor salts solution addition. However, the addition of lanthana avoids the nucleation of α-Al_2O_3 and produces a thermal stabilization of the catalysts decreasing the specific surface area loss ascribed to γ to α alumina transition [37,38].

The XRD patterns of support (a) and prepared catalyst (b) are shown in Fig. 2. The support pattern was ascribed to γ-Al_2O_3 which diffraction peaks match perfectly with the

Please cite this article in press as: Benito M, et al., Ni–Co bimetallic catalyst for hydrogen production in sewage treatment plants: Biogas reforming and tars removal, International Journal of Hydrogen Energy (2015), http://dx.doi.org/10.1016/j.ijhydene.2015.06.163

Table 1 – Textural properties of catalyst synthesized and support.

Textural parameter	Alumina	Catalyst
BET ($m^2 \cdot g^{-1}$)	119.0571	104.0032
v_{pore} ($cm^3 \cdot g^{-1}$)	0.419200	0.349296
Average pore size (nm)	13.59	13.43

reference pattern 00-004-0858 of the JCPDS. Some differences were identified in catalyst sample after support impregnation with the active phase and further thermal stabilization at 800 °C. An important intensity decrease (factor of 5) was detected and may be due to a loss of crystallinity.

It is important to note that there are no evidence of diffraction peaks that could be ascribed to nickel and cobalt species, which indicates the low particle size or the amorphous state. However, some diffraction peaks were shift to lower 2⊙ indicating the formation of new phases after impregnation and calcination. The peak presented at 2⊙ 31,11° could be ascribed to the formation of $LaCoO_3$ (01-086-1665) which intensity increases as cobalt concentration increases (diffractograms doesn't shown). A shift in the peak at 2⊙ 66,99° was identified, and could correspond to the formation of $NiAl_2O_4$ (00-001-1299). This fact was supported by the decrease of the peak intensity that appears at 2⊙ 39,58° ascribed to alumina. The results would be consistent with the existence of strong interaction between the metal and the support (SMSI).

XPS performed on fresh calcined sample shows a surface composition of Ni 3.21 wt%, Co 2.34 wt%, La 2.07 wt%, O 54.02 wt%, C 1.25% and Al 37.11 wt%. The comparison of the composition obtained by XRF and XPS allows having an idea about the amount of element presented on the surface, and the element amount in the bulk, and therefore a dispersion estimation (Table 2). It is important to note that is really difficult to obtain an accurate measure of the dispersion of Ni–Co bimetallic catalysts and catalysts with SMSI effects because of the adsorption in the case of Co particles is activated with the temperature, opposite to Ni particles, being different the optimum probe molecule used for both metal particles dispersion determination [39,40]. It is observed that lanthanum is presented on catalyst surface while a 60% of cobalt and 42.80% of Ni are presented on the surface. Taking into account the species detected in XRD characterisation and chemical analysis results obtained by XRF and XPS it is possible to determine that after calcination at 800 °C a part of Ni and Co has interacted with support.

The curve fitting of Ni 2p ½ and Ni 2p 3/2 (figures doesn't presented) corroborates the presence of $Ni(OH)_2$. The deconvolution of the curve of Co 2p ½ and Co 2p 3/2 allows identifying the presence CoO, $Co(OH)_2$ and Co_2O_3 species.

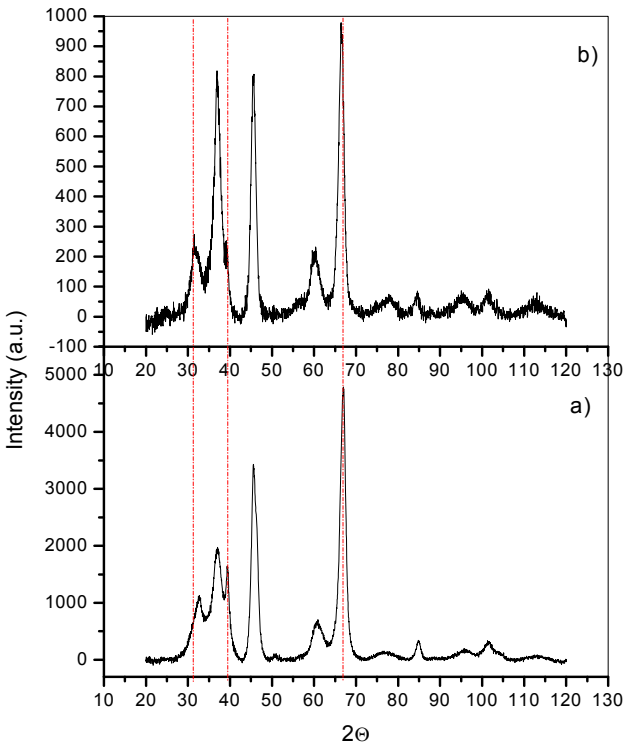

Fig. 2 – Diffractograms obtained on catalytic support (a), and catalytic simple (b).

Catalyst testing

The catalyst synthesized was submitted to a biogas simulated stream with a CH_4:CO_2 ratio of one, and a sewage sludge gasification simulated stream with a toluene model compound concentration of 25 $g \cdot Nm^{-3}$, the highest tar concentration range usually presented in bubble fluidised gasifiers [41,42].

Biogas simulated reforming

Catalytic activity tests. A biogas reaction test in a model biogas stream with a ratio CH_4:CO_2 of one and flow of 20 N $cm^3 \cdot min^{-1}$ was performed in a microactivity reactor. The catalyst sample (200 mg) was tested at W/F mass hourly space velocity of 9.9 mg min· N cm^{-3}, in a temperature range 750–450 °C, decreasing the reaction temperature in 50 °C steps, and maintaining 3 h in every temperature step. Methane, carbon dioxide conversion and products distribution *vs.* temperature for biogas simulated stream (Fig. 3) was determined. It is noteworthy that methane and carbon dioxide conversion achieved equilibrium values predicted by thermodynamic equilibrium in the temperature range studied, equilibrium values determined in a previous paper [45]. Carbon dioxide conversion was higher than methane conversion in the temperature range studied as a consequence of reverse water gas shift reaction (Eq. (2)) and reverse Boudouard reaction (Eq. (3)) contributions [43,44]. The light-off temperature for methane conversion was 620 °C, reaching a conversion of 80% at 750 °C.

Table 2 – Chemical composition of synthesized catalyst determined by XRF and XPS.

Element	Nominal	XRF	XPS	% On surface
C				
Al		41.00	37.11	
Co	3.00	3.90	2.34	60.00
Ni	5.00	7.50	3.21	42.80
La	3.00	1.80	2.07	100

Please cite this article in press as: Benito M, et al., Ni–Co bimetallic catalyst for hydrogen production in sewage treatment plants: Biogas reforming and tars removal, International Journal of Hydrogen Energy (2015), http://dx.doi.org/10.1016/j.ijhydene.2015.06.163

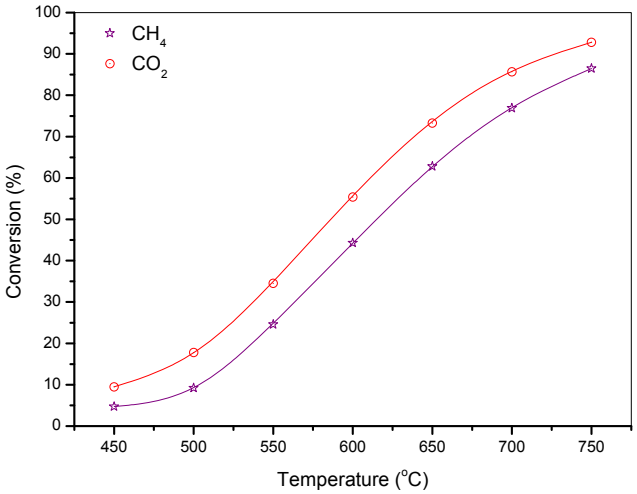

Fig. 3 – Methane and carbon dioxide conversion *vs.* temperature in a biogas simulated catalytic activity test.

$$CH_4 + CO_2 \rightleftharpoons 2CO + 2H_2 \quad \Delta H^\circ = +247\ KJ\ mol^{-1} \tag{1}$$

$$CO + H_2O \rightleftharpoons H_2 + CO_2 \quad \Delta H^\circ = -41\ kJ\ mol^{-1} \tag{2}$$

$$2CO \rightleftharpoons C + CO_2 \quad \Delta H^\circ = +172\ kJ\ mol^{-1} \tag{3}$$

$$CH_4 + H_2O \rightleftharpoons CO + 3H_2 \quad \Delta H^\circ = +206\ kJ\ mol^{-1} \tag{4}$$

$$CH_4 \rightleftharpoons C + 2H_2 \quad \Delta H^\circ = +75\ kJ\ mol^{-1} \tag{5}$$

The Fig. 4 represents the products distribution as a function of temperature. Hydrogen and carbon monoxide concentration increased as temperature increased as a consequence of methane reaction with carbon dioxide (Eq. (1)), supported by methane and carbon dioxide decrease *vs.* temperature. Water concentration starts to increase achieving a maximum at 600 °C as a consequence of reverse water gas shift contribution (Eq. (2)) favoured at high temperature range. At reaction temperature higher than 600 °C, H_2O concentration decreases as a consequence of methane steam reforming reaction contribution (Eq. (4)).

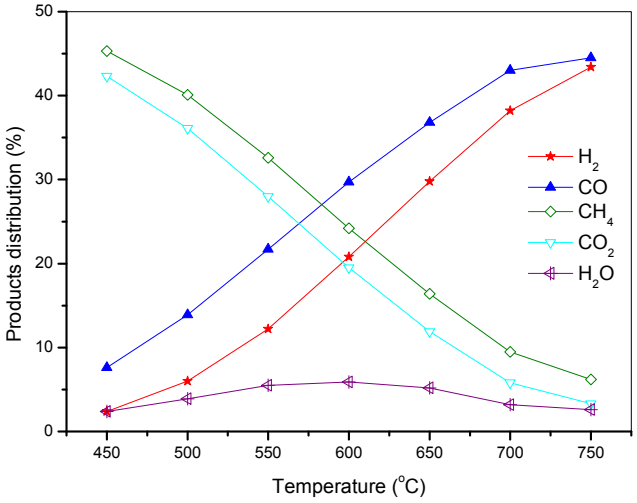

Fig. 4 – Products distribution *vs.* temperature in a biogas simulated catalytic activity test.

In order to study the catalyst performance, a long-term reaction experiment was done at low methane and carbon dioxide conversions, this means in a defect of catalyst mass. With this type of experiment is possible to detect deactivation phenomena that could be masked by the use of an excess of catalyst mass in the reaction test. It is important to remark, that long-term experiments were performed at 700 °C, where coke is thermodynamically favoured, the reaction is kinetically controlled and catalyst really evaluated. A further temperature increase c.a. 800 °C, increases the methane and carbon dioxide (as thermodynamic equilibrium predicts) and carbon deposition rate decreases. However, the thermal contribution in comparison with catalytic one also increases, and the catalyst is evaluated in less restrictive reaction conditions. Fig. 5 represents the conversion of methane and carbon dioxide as a function of time. It is a remarkable fact the stability of methane and carbon dioxide conversion after 95 h in reaction conditions. Ma et al. [44] studied Ni–Co bimetallic catalysts for biogas reforming at 800 °C and WHSV of 10 mg min· N cm^{-3}. The best result was obtained for the catalyst with 7 %wt Ni and 3%wt Co. In order to understand the phenomena involved in catalytic process, it is important to compare parameters such as X_{CH4}/X_{CO2} and H_2/CO with thermodynamic prediction. On the one hand, the X_{CH4}/X_{CO2} value obtained was 0,74, higher than the value predicted by thermodynamic equilibrium (0,62), taking into consideration that X_{CO2} was 0,36 *vs.* 0,47 (equilibrium value). On the other hand, H_2/CO achieved was 0,31 *vs.* 0.53 (equilibrium value). In a previous paper [45], Ni supported on lanthana promoted alumina catalyst was tested in a long-term reaction experiment in the same reaction conditions after 40 h. The X_{CH4}/X_{CO2} value was slightly higher than equilibrium. However, the ratio H_2/CO was much higher than the obtained in Ni–Co lanthana promoted catalyst. Therefore, the addition of

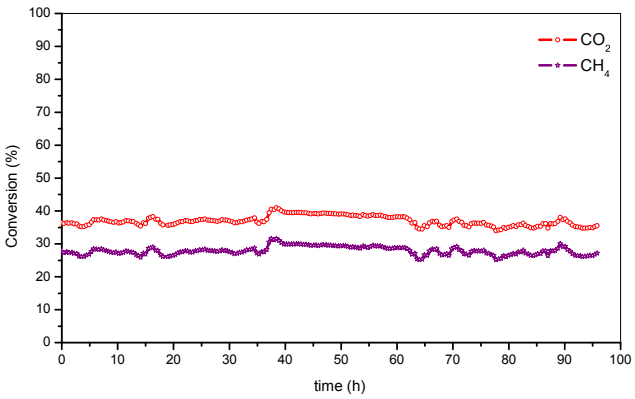

Fig. 5 – Methane and carbon dioxide conversion *vs.* time in a biogas simulated catalytic activity long-term test at 700 °C.

Please cite this article in press as: Benito M, et al., Ni–Co bimetallic catalyst for hydrogen production in sewage treatment plants: Biogas reforming and tars removal, International Journal of Hydrogen Energy (2015), http://dx.doi.org/10.1016/j.ijhydene.2015.06.163

cobalt as a promoter inhibits methane decomposition (Eq. (5)), responsible of carbon formation and the high H_2/CO ratio obtained. The decrease of X_{CO2} could be a consequence of the lower carbon rate formation and therefore the low coke deposits gasification contribution (reverse Boudouard reaction).

Post-reaction catalyst characterisation. The sample submitted to long-term reaction experiments up to 95 h was characterised by temperature programmed oxidation (TPO) and scanning electron microscopy (SEM) in order to detect carbon deposition on catalyst sample. Fig. 6 shows a catalyst SEM image obtained after 95 h in reaction. EDX analysis revealed the lack of carbon deposition on the catalyst particle (Table 3). However, TPO experiment performed on catalytic sample (Fig. 7) revealed the presence of a negligible carbon deposit. The types of carbon deposits were identified depending on carbon oxidation temperature. In this sense, low temperature gasification carbon deposit (525 °C), that could be ascribed to carbon deposited on nickel particles without interaction with catalytic support (C_α), and amorphous carbon deposited on catalytic support (C_β) that was oxidised at 600 °C [46–48] were identified. The mass loss

Table 3 – EDX Analysis performed on catalyst submitted to long-term reaction conditions in biogas reforming.

Element	Weight (%)	Atomic (%)
Al K	80.19	91.36
Co K	3.41	1.78
Ni K	10.71	5.61
La L	5.69	1.26
C K	0.00	0.00

ascribed to carbon deposition in our work was 2.7768%, that represents an average rate of coking of 0.2922 $mg \cdot g_{cat}^{-1} \cdot h^{-1}$. On one hand, Ma et al. [44] determined an average rate of coking of 0.6527 $mg \cdot g_{cat}^{-1} \cdot h^{-1}$ in a 100 h experiment but operating in isothermal conditions at 800 °C with a WHSV ($mL \cdot g_{cat}^{-1} \cdot min^{-1}$), this means 20 times higher. On the other hand, Zhang et al. [49] determined an average rate of coking of 0.2175 $mg \cdot g_{cat}^{-1} \cdot h^{-1}$ in a 2000 h experiment performed at 750 °C, being this value similar to the value obtained in the present work. Not only the value obtained by Zang et al. is similar to the value obtain in this work but also the type of carbon deposited. From this stand point,

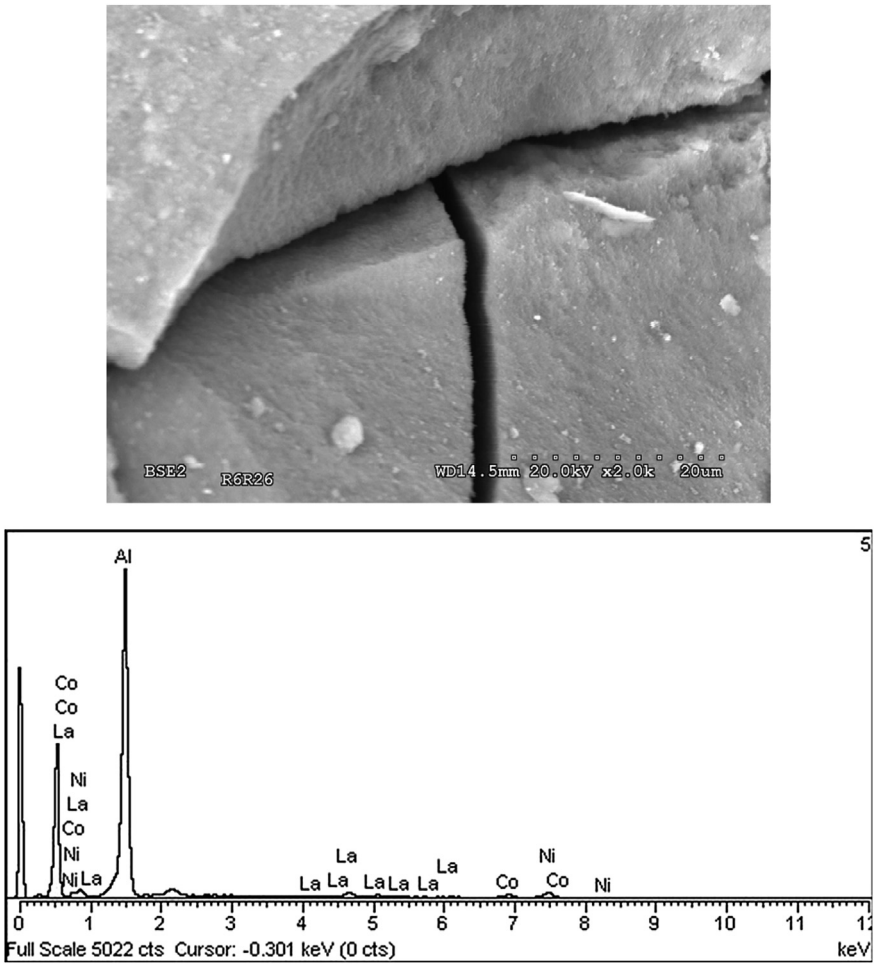

Fig. 6 – Scanning electron microscopy image and EDX spectra of a catalyst sample submitted to 95 h in a biogas conversion test.

Please cite this article in press as: Benito M, et al., Ni–Co bimetallic catalyst for hydrogen production in sewage treatment plants: Biogas reforming and tars removal, International Journal of Hydrogen Energy (2015), http://dx.doi.org/10.1016/j.ijhydene.2015.06.163

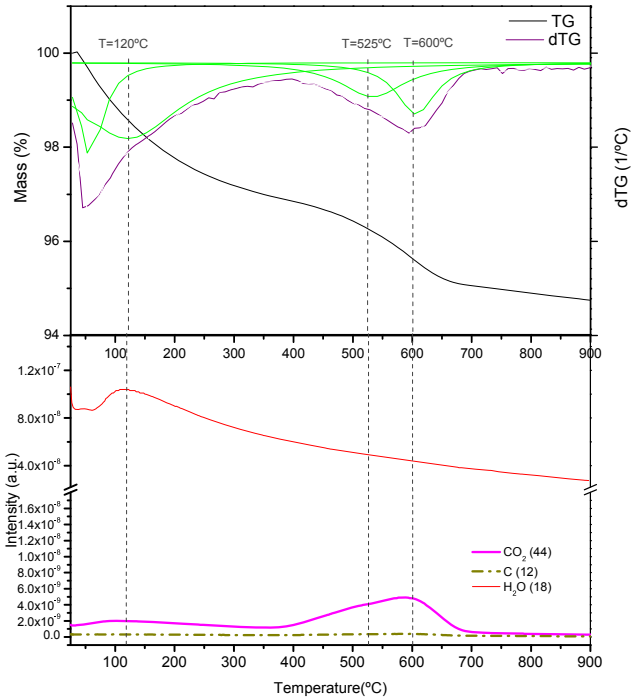

Fig. 7 – TG-mass obtained in a temperature programmed oxidation experiment of a catalyst sample after 95 h in a biogas conversion test.

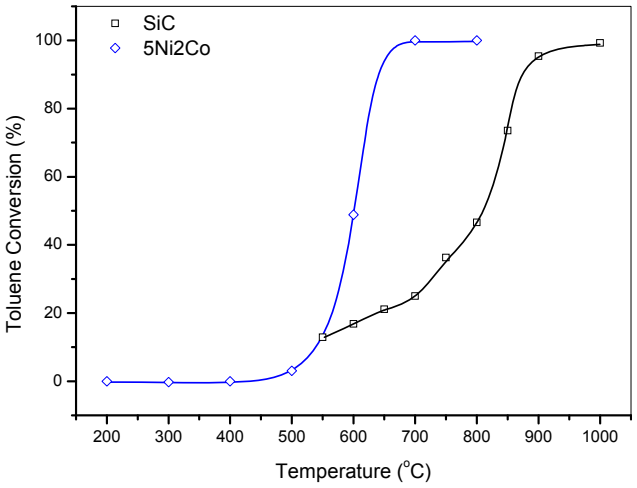

Fig. 8 – Toluene conversion. Catalytic process vs. thermal.

Zang et al. identified two types of carbon that can oxidizes at 500 °C and 600 °C respectively, being the temperature values obtained in this work of 525 °C and 600 °C respectively. The first peak oxidation temperature difference could be ascribed as a consequence of the different Ni/Co ratio used in both works or related to the different interaction between active phase, promotor and support, also different in both cases. No information about carbon oxidation temperature was obtained in the Ma et *al.* article in order to compare it.

Tar conversion in gasification simulated streams

Thermal process. Prior to start with catalytic tests, a thermal toluene conversion process was performed using SiC as inert material as substitute of catalytic sample in the tube reactor, in order to have a reference to study the catalytic process. The light-off temperature, at which 50% of conversion is reached, for thermal cracking process was closed to 815 °C (Fig. 8) when a gasification gas was applied, being necessary a temperature of 1000 °C to complete toluene conversion.

Thermal conversion of toluene led to the formation of some by-products. The number of by-products was increased when reaction temperature was decreased. A total of twenty-one by-products were identified and quantified by mass spectrometry (Table 4). The main by-products at 1000 °C were benzene, due to the loss of the methyl group of toluene, and naphthalene due to the condensation of two aromatic rings. The temperature decrease up to 900 °C resulted in lower conversion of toluene and a rise in the number and concentration of by-products such as benzene, naphthalene, phenanthrene, biphenyl, biphenylene and anthracene. At 850 °C, the increase in concentration and number of by-products was higher, especially in the heaviest compounds such as fluorene, phenanthrene, anthracene and fluoranthene. Below 600 °C the conversion of toluene was so small that only benzene was formed.

Catalytic activity tests. The synthesized catalyst sample was also tested for tar model (toluene) conversion in the upgrading of air sludge gasification streams. For this propose, 1750 mg of catalytic sample with particle size range 0.5–1.0 mm was introduced in a 3/8″ o.d tube reactor. The catalyst operated at W/F of 16.6 mg min·N cm^{-3}. The Fig. 9 compiles toluene conversion and by-products distribution *vs.* temperature. The light-off temperature for toluene conversion was 600 °C (Fig. 9 a), this means 215 °C lower than thermal process, achieving total toluene conversion at 700 °C *vs.*1000 °C obtained in the thermal process. The light-off temperature for toluene conversion coincides with the temperature at which benzene reaches the maximum concentration (Fig. 9b), being benzene the only by-product obtained. The behaviour of benzene concentration curve is typical of a reaction intermediate, being the loss of methyl group the first reaction step of the reaction mechanism that could tentatively proposed for this catalyst operation. This aspect will be studied in depth in upcoming papers using the technique of *in situ* FTIR-DRIFTS.

It is noteworthy the selectivity achieved with the catalyst synthesized in comparison with the thermal process. The catalyst is capable of converting benzene and methane into hydrogen and carbon monoxide, avoiding the reactions that lead to benzene condensation products such as complex tar (naphthalene, phenanthrene, biphenyl, biphenylene, anthracene …) identified and quantified in the thermal process (figures does not shown).

Please cite this article in press as: Benito M, et al., Ni–Co bimetallic catalyst for hydrogen production in sewage treatment plants: Biogas reforming and tars removal, International Journal of Hydrogen Energy (2015), http://dx.doi.org/10.1016/j.ijhydene.2015.06.163

Table 4 – Tar concentration vs. temperature obtained in the thermal process with a simulated sewage sludge gasification stream.

Compound ($g \cdot m^{-3}$)	Reaction temperature (°C)					
	1000	900	850	800	700	600
Benzene	11.525472	6.897459	12.424386	8.021426	0.684999	0.092947
Toluene	0.188289	0.462023	6.495409	14.845699	18.725077	21.390684
Ethyl cyclohexane					0.000462	0.003392
Ethyl benzene			0.002988	0.007400	0.007727	0.007135
m + p-xylene		0.001238	0.027595	0.037334	0.003105	0.000920
Styrene	0.001476	0.000194	0.001200	0.001638	0.000157	
o-xylene		0.000248	0.009062	0.014671	0.001233	
Indene	0.007859	0.000791	0.000965	0.000491	0.000031	
Naphthalene	0.087762	0.001117	0.000473	0.000144		
1-methyl naphthalene	0.000355	0.000090				
2-methyl naphthalene	0.000230	0.000061				
biphenyl	0.012930	0.016936	0.004321	0.001136		
2,2′-dimethyl biphenyl	0.000082	0.000085	0.000147	0.000136	0.000073	
biphenilene	0.030369	0.000992	0.000155	0.000057		
4-methyl-1,1′biphenyl	0.000144	0.000157	0.001445	0.000686		
Acenaphtilene			0.000313	0.000147		
acenaphtene	0.000252					
3,4′-dimethyl-1,1′-biphenyl			0.000032	0.000079		
Fluorene	0.000523	0.001004	0.000442	0.000199		
Phenantrene	0.003779	0.000819	0.000083	0.000085	0.000015	
Antracene	0.000486	0.000298	0.000049	0.000056	0.000019	
2-phenyl naphthalene		0.000230				
Pyrene	0.000095	0.000344				
Fluorantene	0.000100	0.000212	0.000126			

The Fig. 9 c represents the main products concentration as a function of temperature. Up to 600 °C main products concentration remains constant. When temperature was increased, CO concentration starts to increase and CO_2 starts to decrease simultaneously. The slight increase in the hydrogen concentration despite the increase in the CO_2 conversion (RWGS) put in evidence the greater contribution of the methane reforming reaction, thermodynamically favoured in this temperature range. It is also important to note that the catalyst is capable of converting methane at temperature higher than 700 °C, very important aspect if the aim is to apply the catalytic system to hydrogen production. In this reaction the catalytic support plays an important role on reaction mechanism. From this point of view, parameters such as surface acidity, surface area, pore structure … can affect the catalyst activity [50]. Maximizing catalytic activity is not the only goal for tar conversion. The catalyst stability is crucial for industrial application. Sutton et al. [51] studied a Ni/Al_2O_3 alumina catalyst that gave the highest activity for tar removal but it was not stable [52]. However, surface acidity of alumina as well as nickel ability for C–C and C–H bonds activation is responsible of coke formation and catalyst deactivation. The catalyst synthesized tries to overcome these effects modifying surface acidity by lanthanum basic oxide addition, and controlling nickel activity modifying electronic density of nickel particles by cobalt interaction.

Taking into consideration catalytic gas upgrading system integration in gasification process, reaction temperature at which the catalyst is capable of operating with enough activity and stability is the key factor to maximize the process efficiency. From this point of view, most of Ni/Al_2O_3 catalysts studied in literature used to work at temperature higher than 800 °C [53]. In this temperature range the overall process efficiency including gasification and gas upgrading starts to decrease as hot gas cleaning process temperature increases. Furthermore, the possibility of identifying thermal and catalytic contribution in the process is so difficult. Therefore it is important to develop catalysts capable of working at temperature below gasification process in order to maximize energy efficiency. In this temperature range, the role of the catalysts is really important due to thermal contribution is really low. In this sense, the catalyst synthesised is able to operate at 700 °C with total toluene conversion, this means 100–150 °C lower than gasification temperature.

Long-term catalytic activity tests. A long-term isothermal reaction test at 700 °C maintaining W/F, was performed with the aim of studying the stability and possible deactivation processes in the catalyst synthesized. The Fig. 10 represents toluene conversion *vs.* time. A stabilization time period of 1.5 h was observed due to the influence of reducing medium, where catalyst sample was activated (Fig. 10 a). It is important to note the lack of by-products in the time range studied (Fig. 10 b). In the Fig. 10 c, changes in main products concentrations were observed. On one hand, a reversal in concentrations of carbon dioxide and carbon monoxide due to the contribution of the reverse water gas shift reaction was observed. On the other hand, after catalyst activation period, total methane conversion was achieved, also detected by the increase of hydrogen concentration.

Please cite this article in press as: Benito M, et al., Ni–Co bimetallic catalyst for hydrogen production in sewage treatment plants: Biogas reforming and tars removal, International Journal of Hydrogen Energy (2015), http://dx.doi.org/10.1016/j.ijhydene.2015.06.163

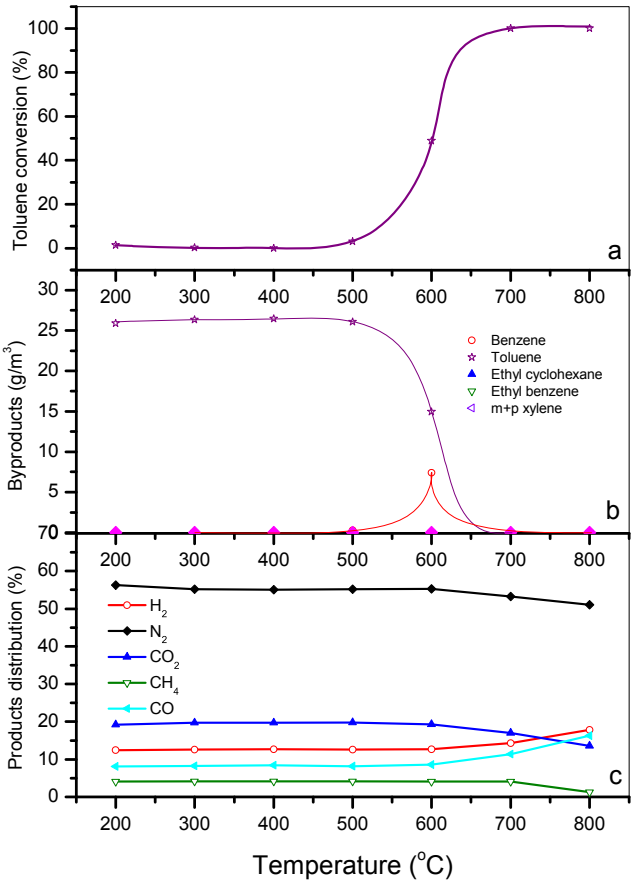

Fig. 9 – Catalytic activity test performed in a tar conversion experiment: a) toluene conversion *vs.* temperature, b) by-product concentration vs. temperature, c) Main products distribution vs. temperature.

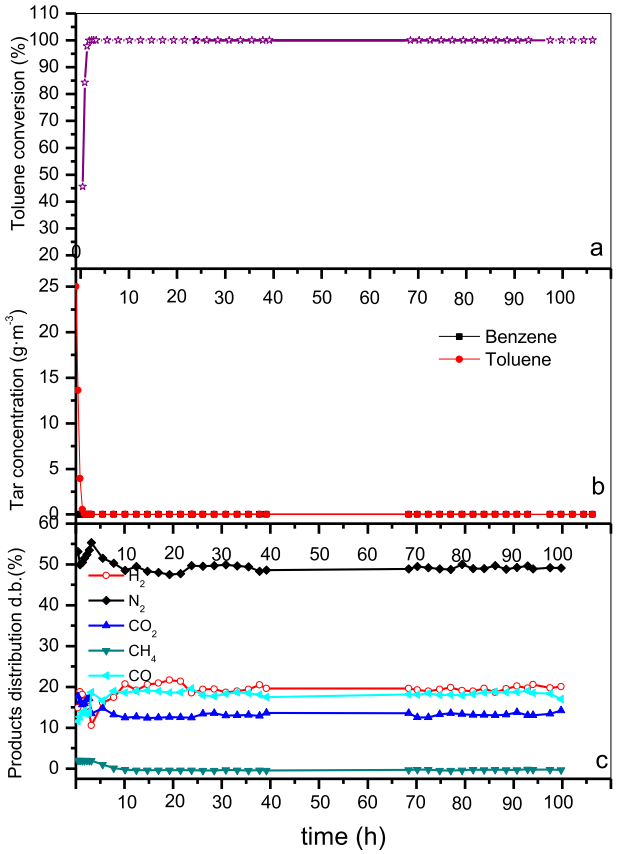

Fig. 10 – Catalytic long-term tar conversion test at 700 °C: a) toluene conversion *vs.* time, b) by-product concentration vs. time, c) Main products distribution vs. time.

Post-reaction catalyst characterisation. Following the same experimental procedure as in the case of methane reforming with carbon dioxide, SEM images of the catalyst sample after 100 h in reaction condition were obtained. In the Fig. 11 catalyst particles with a magnification of 4000x are shown. There are not signals of carbon fibres. EDX analysis performed in different zones of the sample demonstrates the lack of carbon deposits on catalyst particles (Table 5). These results were confirmed by XPS analysis performed on the same catalyst sample. Catalytic sample was also submitted to TPO analysis by TG-mass analysis technique (Fig. 12). The dTG curve (Fig. 11 a) magnified shows the presence of two incipient peaks at 358 °C and 547 °C that could be ascribed to coke deposits gasification. However, mass spectroscopy analysis performed simultaneously doesn't show any desorption peak of *m/z* 44 ascribed to carbon dioxide which put in evidence that coke deposition after 100 h in reaction conditions was negligible.

Conclusions

This work was focused on the possibility of applying the same concept in catalyst design to be implemented in two thermal processes involved in sewage treatments plants for energy valorisation for hydrogen production: biogas direct reforming (carbon dioxide methane reforming) and tar conversion in sewage sludge gasification. The catalyst deactivation phenomena in both processes was coke deposition on catalyst surface, and the strategy to overcome it proposed in this work was the same.

Catalyst designed and synthesized achieved equilibrium values predicted by thermodynamic equilibrium for direct carbon dioxide methane reforming. The catalyst tested in long-term experiments up to 95 h demonstrated total stability in methane and carbon dioxide conversion as well as products distribution.

On the other hand, catalyst tests in model gasification streams showed total toluene and methane conversion without by-products (tar) formation, levels maintained in the long-term experiments.

Post-reaction catalyst samples characterisation by SEM, TPO and XPS demonstrated the lack of carbon deposits responsible of catalyst deactivation which corroborates the stability of the reaction tests. The results obtained allow the scale up of both processes to have and integral solution for hydrogen production from sewage treatment plants.

Please cite this article in press as: Benito M, et al., Ni–Co bimetallic catalyst for hydrogen production in sewage treatment plants: Biogas reforming and tars removal, International Journal of Hydrogen Energy (2015), http://dx.doi.org/10.1016/j.ijhydene.2015.06.163

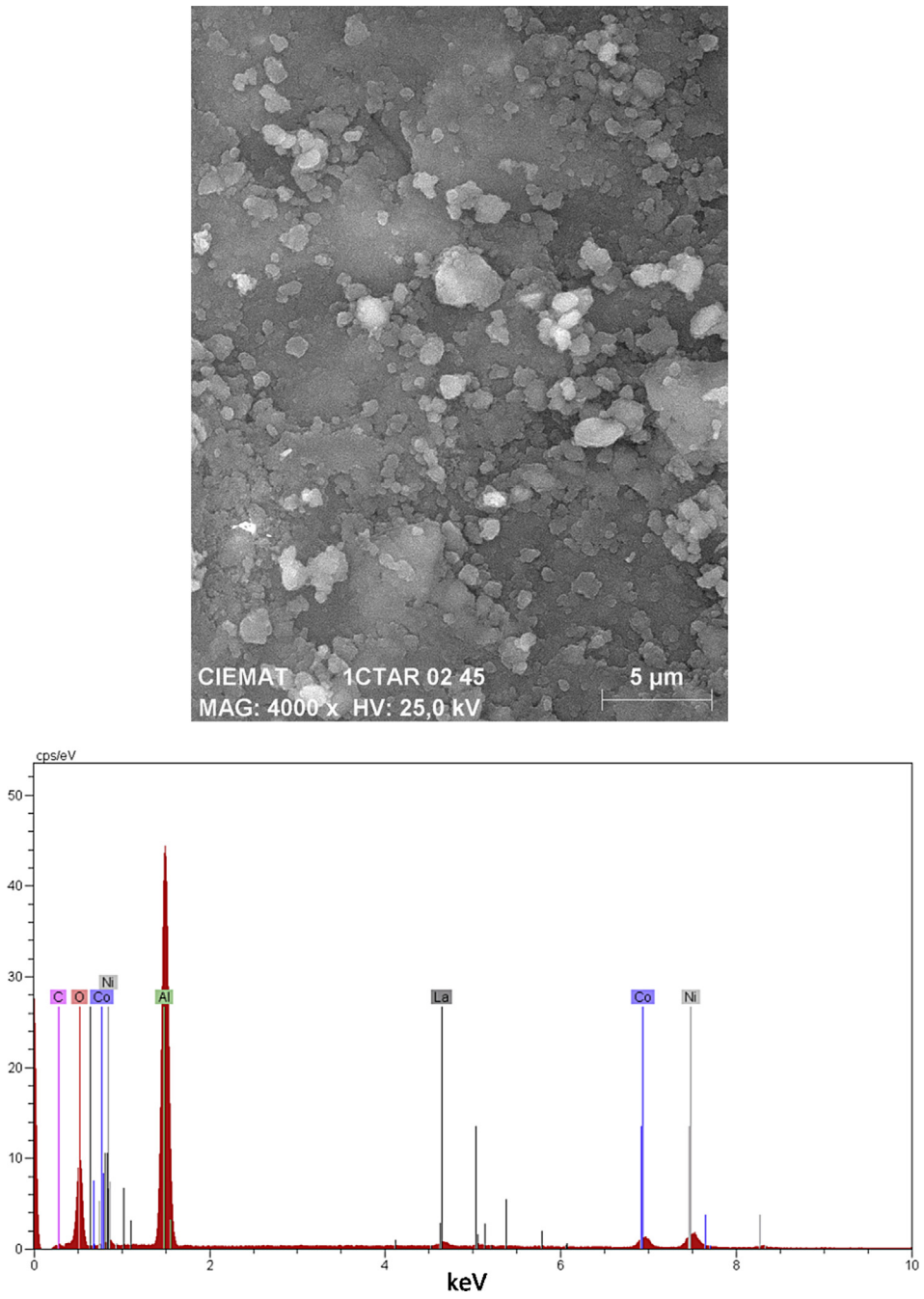

Fig. 11 – Scanning electron microscopy image and spectra of a catalyst sample submitted to 95 h in a toluene conversion test.

Please cite this article in press as: Benito M, et al., Ni–Co bimetallic catalyst for hydrogen production in sewage treatment plants: Biogas reforming and tars removal, International Journal of Hydrogen Energy (2015), http://dx.doi.org/10.1016/j.ijhydene.2015.06.163

Table 5 – EDX Analysis performed on catalyst submitted to long-term reaction conditions in tar conversion.

Element	Weight (%)	Atomic (%)
Al K	83.24	92.14
Co K	5.44	2.79
Ni K	8.19	4.38
La L	3.11	0.68
C	0.0	0.0

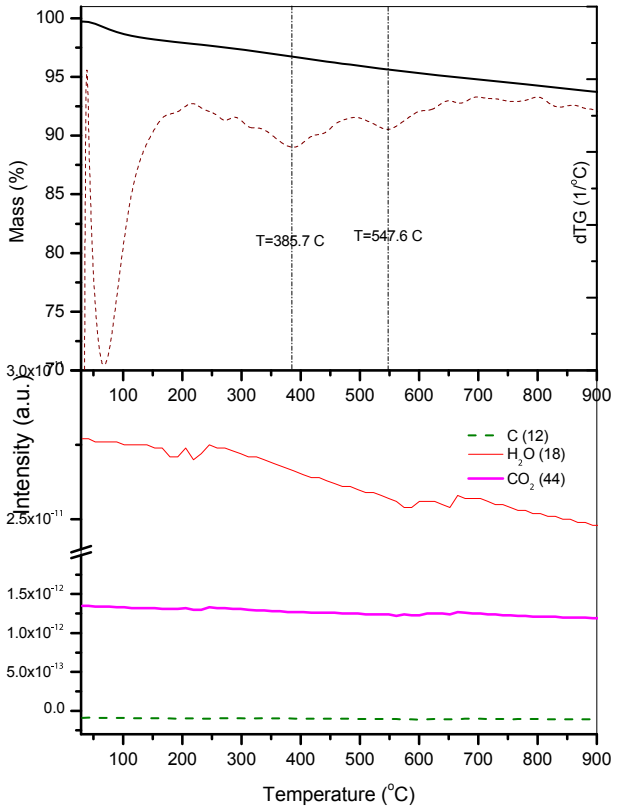

Fig. 12 – TG-mass obtained in a temperature programmed oxidation experiment of a catalyst sample after 95 h in a tar conversion test.

Acknowledgements

This work was is a scientific result of the Project CATARSYS ENE2012-36299 entitle: 'Development of Active, Selective and Stable Tar Reforming Catalysts for Upgrading of Biomass and Waste Gasification Streams', financed by State Secretariat for Research, Development and Innovation (Spanish Ministry of Economy and Competitiveness).

REFERENCES

[1] Barometre Biogaz-EUROBSERV'ER-DÉCEMBRE 2012. Systemes solaires: Le journal des energies renouvelables, vol. 212; 2012.
[2] Hawkes AD. In: (Ed) RB, editor. Tecno-economic assesment of small and microcombined heat and power (CHP) systems, tecno-economic assesment of small and microcombined heat and power (CHP) systems. Oxford: Woodhead Publishing Limited; 2011. p. 60–8.
[3] Sacco Jr A, Geurts FWAH, Jablonski GA, Lee S, Gately RA. Carbon deposition and filament growth on Fe, Co, and Ni foils using CH_4, H_2 ,H_2O, CO ,CO_2 gas mixtures. J Catal 1989;119:322–41.
[4] Wolf EE, Alfani F. Catalysis deactivation by coking. Catal Rev Sci Eng 1982;24:329–71.
[5] Vogt ETC, van Dillen AJ, Geus JW. Prevention of growth of filamentary carbon in supported iron and nickel catalysts. In: Froment BDAGF, editor. Studies in surface science and catalysis, catalyst deactivation 1987 Proceedings of the 4th International Symposium. Elsevier; 1987. p. 221–33. E.T.C. Vogt, A. J. van Dillen, J.W. Gens, Stud. Surf. Sci. (1987) 221.
[6] Williams DS, Möller R, Grabke HJ. High Temp. Sci 1981;14(33).
[7] Ross JRH, van Keulen ANJ, Hegarty MES, Seshan K. Catalysis today. In: Proceedings of the 1st global conference of Young Chinese Scientist on catalysis science and technology30; 1996. p. 193–9.
[8] Rostrup-Nielsen JR, Sehested J, NÃ¸rskov JK. Hydrogen and synthesis gas by steam- and CO_2 reforming. Adv Catal 2002:65–139. Academic Press.
[9] Rostrup Nielsen JR, Rostrup Nielsen T. Cattech 6 150. 2002.
[10] Vita A, Pino L, Cipitì F, Laganà M, Recupero V. Biogas as renewable raw material for syngas production by tri-reforming process over $NiCeO_2$ catalysts: optimal operative condition and effect of nickel content. Fuel Process Tech 2014;127:47–58.
[11] Izquierdo U, Barrio VL, Bizkarra K, Gutierrez AM, Arraibi JR, Gartzia L, et al. Ni and Rh single bond Ni catalysts supported on Zeolites L for hydrogen and syngas production by biogas reforming processes. Chem Eng J 2014;238(15):178–88.
[12] Muradov N, Smith F, T-Raissi A. Hydrogen production by catalytic processing of renewable methane-rich gases. Int J Hydrogen Energy 2008;33:2023–35.
[13] Ferreira-Aparicio P, Benito M, Sanz JL. New trends in reforming technologies: from hydrogen industrial plants to multifuel microreformers. Catal Rev Sci Eng 2005;47:1–99.
[14] Edwards JH, Maitra AM. The chemistry of methane reforming with carbon dioxide and its current and potential applications. Fuel Process Technol 1995;42(2–3):269–89.
[15] Bradford MCJ, Vannice MA. CO_2 reforming of CH_4. Catal Rev Sci Eng 1999;41(1):1–42.
[16] Rostrup-Nielsen JR, Sehested J, Nørskov JK. Hydrogen and synthesis gas by steam- and CO_2 reforming. Adv Catal 2002;47:65–139.
[17] Tokunaga O, Osada Y, Ogasawara S. Reduction of carbon dioxide with methane over Ni-catalyst. Fuel 1989;68:990–4.
[18] Rostrup-Nielsen J, Trimm DL. Mechanisms of carbon formation on nickel-containing catalysts. J Catal 1977;48(1–3):155–65.
[19] Schulz LA, Kahle LCS, Herrera Delgado K, Schunk SA, Jentys A, Deutschmann O, et al. On the coke deposition in dry reforming of methane at elevated pressures. Appl Catal A Gen 2015 [In Press].
[20] Gadalla AM, Bower B. The role of catalyst support on the activity of nickel for reforming methane with CO_2. Chem Eng Sci 1988;43:3049–62.
[21] Gil-Lalaguna N, Sánchez JL, Murillo MB, Ruiz V, Gea G. Use of sewage sludge combustion ash and gasification ash for high-temperature desulphurization of different gas streams. Fuel 2014;129:147–55.
[22] Anis S, Zainal ZA. Tar reduction in biomass producer gas via mechanical, catalytic and thermal methods: a review. Renew Sustain Energy Rev 2011;15:2355–77.

[23] Han J, Kim H. The reduction and control technology of tar during biomass gasification/pyrolysis: an overview. Renew Sustain Energy Rev 2008;12:397–416.
[24] Devi L, Ptasinski KJ, Janssen FJJG. A review of the primary measures for tar elimination in biomass gasification processes. Biomass Bioenergy 2003;24:125–40.
[25] Xu CC, Donald J, Byambajav E, Ohtsuka Y. Recent advances in catalysts for hot-gas removal of tar and NH_3 from biomass gasification. Fuel 2010;89:1784–95.
[26] Devi L, Craje M, Thüne P, Ptasinski KJ, Janssen FJJG. Olivine as tar removal catalyst for biomass gasifiers: catalyst characterization. Appl Catal A Gen 2005;294:68–79.
[27] Kuhn JN, Zhao Z, Felix LG, Slimane RB, Choi CW, Ozkan US. Olivine catalysts for methane- and tar-steam reforming. Appl Catal B Environ 2008;81:14–26.
[28] Srinakruang J, Sato K, Vitidsant T, Fujimoto K. A highly efficient catalyst for tar gasification with steam. Catal Commun 2005;6:437–40.
[29] Di Felice L, Courson C, Foscolo PU, Kiennemann A. Iron and nickel doped alkaline-earth catalysts for biomass gasification with simultaneous tar reformation and CO_2 capture. Int J Hydrogen Energy 2011;36:5296–310.
[30] Aznar MP, Corella J, Delgado J, Lahoz J. 1. Improved steam gasification of lignocellulosic residues in a fluidized bed with commercial steam reforming catalysts. Indus Eng Chem Res 1993;32:1–10.
[31] Baker EG, Mudge LK, Brown MD. Steam gasification of biomass with nickel secondary catalysts. Indus Eng Chem Res 1987;26:1335–9.
[32] Łamacz A, Krzton A, Djéga-Mariadassou G. Steam reforming of model gasification tars compounds on nickel based ceria-zirconia catalysts. Catal Today 2011;176:347–51.
[33] Łamacz A, Krztoń A, Musi A, Costa P. Reforming of model gasification tar compounds. Catal Lett 2009;128:40–8.
[34] Furusawa T, Saito K, Kori Y, Miura Y, Sato M, Suzuki N. Steam reforming of naphthalene/benzene with various types of Pt- and Ni-based catalysts for hydrogen production. Fuel 2013;103:111–21.
[35] Qiu M, Li Y, Wang T, Zhang Q, Wang C, Zhang X, et al. Upgrading biomass fuel gas by reforming over Ni-MgO/g-Al2O3 cordierite monolithic catalysts in the lab-scale reactor and pilot-scale multi-tube reformer. Appl Energy 2011;90:3–10.
[36] Dou B, Gao J, Sha X, Baek SW. Catalytic cracking of tar component from high-temperature fuel gas. Appl Therm Eng 2003;23:2229–39.
[37] Schaper H, Doesburg EBM, Van Reijen LL. The influence of lanthanum oxide on the thermal stability of gamma alumina catalyst supports. Appl Catal 1983;7:211–20.
[38] Navarro RM, Alvarez-Galvan MC, Rosa F, Fierro JLG. Hydrogen production by oxidative reforming of hexadecane over Ni and Pt catalysts supported on Ce/La-doped Al_2O_3. Appl Cat A Gen 2006;297(1):60–72.
[39] Duchet J-C, Lavalley J-C, Housni S, Ouafi D, Bachelier J, Lakhdar M, et al. Carbon monoxide and oxygen chemisorption and functionalities of sulphided Ni-W/Al_2O_3 hydrotreating catalysts. Catal Today 1988;4:71–96.
[40] Tsai Y-T, Goodwin Jr JG. Comparison of chemisorption close to ambient vs. under reaction conditions for group VIII metal catalysts. J Catal 2011;281:128–36.
[41] Milne TA, Evans RJ. Biomass gasifiers tars: their nature, formation and conversion. NREL 1998. TP-570-25357.
[42] Good J, Ventress L, Zielke U, Van de Kamp W, Sjöström K, Unger C, et al. Sampling and analysis of tar and particles in biomass producer gases. Technical report. 2005.
[43] Bradford MCJ, Vannice MA. Catalytic reforming of methane with carbon dioxide over nickel catalysts II: reaction kinetics. Appl Catal A Gen 1996;142:97–122.
[44] Xu J, Zhou W, Zhaojing L, Wang J, Ma J. Biogas reforming for hydrogen production over nickel and cobalt bimetallic catalysts. Int J Hydrogen Energy 2009;34:6646–54.
[45] Benito M, García S, Ferreira-Aparicio P, Serrano LG, Daza L. Development of biogas reforming Ni-La-Al catalysts for fuel cells. J Power Sources 2007;169:177–83.
[46] Figueiredo JL, Órfao JJM. Carbon deposits on metal catalysts – mechanisms of formation and gasification. Catal Today 1989;5:385–93.
[47] McCarty JG, Wise H. Hydrogenation of surface carbon on alumina-supported nickel. J Catal 1979;57:406–16.
[48] Davis SM, Zaera F, Somorjai GA. The reactivity and composition of strongly adsorbed carbonaceous deposits on platinum. Model of the working hydrocarbon conversion catalyst. J Catal 1982;77:439–59.
[49] Zhang J, Wang H, Dalai AK. Development of stable bimetallic catalysts for carbon dioxide reforming of methane. J Catal 2007;249:300–10.
[50] Yung MM, Jablonski WS, Magrini-Bair KA. Review of catalytic conditioning of biomass-derived syngas. Energy Fuels 2009;23:1874–87.
[51] Sutton D, Kelleher B, Doyle A, Ross JRH. Investigation of nickel supported catalysts for the upgrading of brown peat derived gasification products. Bioresour Technol 2001;80:111–6.
[52] Srinakruang J, Sato K, Vitidsnt T, Fujimoto K. Highly efficient sulfur and coking resistance catalyst for tar conversión with steam. Fuel 2006;85:2419–26.
[53] Simell PA, Hepola JO, Krause AOI. Effects of gasification gas components on tar and amonia decomposition over hot gas clean up catalysts. Fuel 1997;76:1117–27.

Please cite this article in press as: Benito M, et al., Ni–Co bimetallic catalyst for hydrogen production in sewage treatment plants: Biogas reforming and tars removal, International Journal of Hydrogen Energy (2015), http://dx.doi.org/10.1016/j.ijhydene.2015.06.163